Thursday, 23 September 2010

# Relativistic microburst storm characteristics: combined satellite and ground-based observations

Sarah Dietrich and Craig J. Rodger

Department of Physics, University of Otago, Dunedin, New Zealand

Mark A. Clilverd

Physical Sciences Division, British Antarctic Survey (NERC), Cambridge, United Kingdom

Jacob Bortnik

Department of Atmospheric and Oceanic Sciences, University of California, Los Angeles, California, USA

Tero Raita

Sodankylä Geophysical Observatory, University of Oulu, Sodankylä, Finland

**Abstract.** We report a comparison of SAMPEX detected relativistic electron microbursts and short-lived subionospheric VLF perturbations termed FAST events, observed at Sodankylä Geophysical Observatory, Finland, during 2005. We show that only strong geomagnetic disturbances can produce FAST events, which is consistent with the strong link between storms and relativistic microbursts. Further, the observed FAST event perturbation decay times were consistent with ionospheric recovery from bursts of relativistic electron precipitation. However, the one-to-one correlation in time between microbursts and FAST events was found to be very low (~1%). We interpret this as confirmation that microbursts have small ionospheric footprints, and estimate the individual precipitation events to be <4 km radius. In contrast, our study strongly suggests that the region over which microbursts occur during storm event

periods can be at least ~90° in longitude (~6 hours in MLT). This confirms earlier estimates of microburst storm size, suggesting that microbursts could be a significant loss mechanism for radiation belt relativistic electrons during geomagnetic storms. Although microbursts are observed at a much higher rate than FAST events, the ground-based FAST event data can provide additional insight into the conditions required for microburst generation and the time variation of relativistic precipitation.

## 1. Introduction

The dynamics of Earth's Van Allen radiation belts are governed by a number of competing acceleration and loss mechanisms. Particle fluctuation often coincides with a period of disturbance caused by a geomagnetic storm, with the outer belt flux frequently decreasing during storm onset, followed by a gradual repopulation during the recovery period [*Baker et. al*., 1986; *Li et. al*., 1997]. However, this is not always the case; *Reeves et. al*. [2003] found that the post-storm outer belt relativistic electron flux levels can increase (seen to occur for 53% of events studied), decrease (19%) or have no significant change (28%), relative to pre-storm levels. The flux of the outer belt relativistic electron population at geostationary orbits, defined as having energies >1 MeV, is seen to drop over a period of hours during geomagnetic storms [*Onsager et. al*., 2002]. Multiple mechanisms may contribute to these decreases and it has been shown that losses to the atmosphere are likely to be a contributing factor [*Green et. al*., 2004; *Clilverd et al.*, 2006].

Numerical modeling predicts Relativistic Electron Precipitation (REP) to penetrate into the atmosphere to altitudes of 40-60 km, lower altitudes than most other magnetospheric particles are able to reach [*Baker et al*., 1987; *Callis et al*., 1991], depositing large enough amounts of energy so as to dominate all other ionisation sources at this altitude range. REP events can occur across a wide range of timescales, lasting from minutes to hours, or taking the form of a brief microburst (<1 s) of precipitating electrons. The occurrence of relativistic microbursts has been studied since they were first reported by *Brown and Stone* [1972], but there are still significant unknowns. The first reports of relativistic microbursts (as distinct from those in the tens of keV range) appear to have been made by the S81-1 satellite [*Imhoff et al.*, 1992]. Observations from the Solar Anomalous Magnetospheric Particle Explorer (SAMPEX) have helped to determine some characteristics of REP microbursts, showing that they are spatially small [*Blake et. al*.,

1996]. *Nakamura et. al*. [2000] found that microbursts tend to occur during storm time in the local dawn sector and are likely to be produced through interactions with electron whistler-mode waves. Microburst production has also been linked to interaction with chorus waves [*Lorentzen et. al*., 2001a; *O'Brien et. al*., 2004; *Bortnik and Thorne*, 2007], which occur predominantly in the dawn sector. The majority of geomagnetic storms show a sharp increase in microburst activity, tending to occur at lower *L* during the storm onset, then slowly moving outward during the recovery period [*Johnston and Anderson*, 2010; *Nakamura et. al*., 2000]. At this stage it is unclear from spacecraft data how large a spatial region is affected when relativistic microbursts take place. However, estimates have shown that relativistic microbursts could totally deplete the relativistic electron population of the outer belt during a geomagnetic storm [*Lorentzen et al*., 2001b; *O'Brien et. al*., 2004]. Further information is required to understand the nature of magnetospheric relativistic electron losses [*Thorne et al.*, 2005], requiring additional (and preferably) simultaneous measurements of microburst characteristics.

As there are many suggestions but little certainty about the behavior of microbursts, methods of sensing REP at its lowest penetration altitude would be advantageous. Ionisation levels at the 40-60 km altitude range can be difficult to probe, with one of the few effective monitoring techniques being the use of long-range Very Low Frequency (VLF) signals. VLF waves propagate by reflecting between the Earth's surface and the lower edge of the ionosphere, travelling in what is effectively an Earth-ionosphere waveguide. The altitude of the lower boundary of the ionosphere varies with solar zenith angle and local geomagnetic conditions, having an approximate value of 70-85 km. Hence, REP tends to penetrate to below the lower ionospheric boundary, causing a pronounced increase in ionospheric ionization in the region of the precipitation event. Any VLF signal whose propagation path passes through the ionization change region will be perturbed in amplitude and phase, and as a result imprinted with an

77 indication of REP activity. Recent studies of subionospheric VLF signals have found
78 perturbation signatures of ~1 s to occur during periods of geomagnetic disturbance [*Clilverd et.*
79 *al*., 2006; *Rodger et. al*., 2007]. These perturbations have been termed FAST events and are
80 thought to be the first documented ground-based detection of REP microbursts. It is
81 hypothesized that each FAST event is the signature of one microburst, with a "rainstorm" of
82 multiple microburst “raindrops” occurring in the area local to the receiver.

83 In this paper we make a comparison between the characteristics of FAST events detected by
84 subionospheric VLF and microbursts detected on a satellite, to determine the validity of the
85 hypothesis that FAST events are the subionospheric signature of relativistic electron microburst
86 precipitation events. Correlations in space and time will be examined to determine as much as
87 possible about the nature of FAST events and to expand upon what is currently known about
88 microbursts. In particular, the potential size of a single REP microburst, or “raindrop” size, is
89 investigated, as is the size of the region across which microbursts can occur simultaneously, the
90 "rainstorm" size.

91 **2. Instrumentation**

92 This study combines subionospheric VLF signals and satellite data recorded from December
93 2004 – June 2005. We examine subionospheric VLF data detected at a VLF receiver located at
94 the Sodankylä Geophysical Observatory (SGO), in Finland (67.4ºN, 26.4ºE, *L*=5.3). We use
95 signals from transmitters located in Europe and North America, i.e., NDK (46.4º N, 98.3º E,
96 *L*=3.3; North Dakota, USA; 25.2 kHz), NAA (44.6º N, 67.3ºE, *L*=2.9; Maine, USA; 24.0 kHz),
97 NRK (64.2º N, 21.9º W, *L*=5.6; Keflavik, Iceland; 37.5 kHz), DHO (53.1º N, 7.6º W, *L*=2.4;
98 Ramsloh, Germany; 23.4 kHz) and ICV (40.9º N, 9.8º W, *L*=1.5; Tavolara Island, Italy;
99 20.27 kHz). The transmitter locations and their signal transmission paths to SGO are shown in
100 Figure 1. The SGO VLF receiver is part of the Antarctic-Arctic Radiation-belt Dynamic

Deposition VLF Atmospheric Research Konsortia (AARDDVARK) network. Further information about the AARDDVARK network can be found in *Clilverd et. al.* [2009a], and the AARDDVARK website at http://www.physics.otago.ac.nz/space/AARDDVARK_homepage.htm.

The Solar Anomalous and Magnetospheric Particle Explorer (SAMPEX) satellite carries the Heavy Ion Large Telescope (HILT), which gives high sensitivity and 30 ms time resolution measurements of the flux of >1.05 MeV electrons [*Klecker et. al.*, 1993]. While the Si-Li detectors are dominated by relativistic electrons during passes through the outer radiation belt, they may also be contaminated by protons during solar proton events. Monte Carlo calculations predict that 1 MeV electrons see the HILT as having an effective geometric factor of ~100 $cm^2sr$ [*Blake et al.*, 1996; *Nakamura et al.*, 1998], a substantial viewing window that is ideal for studying energetic electron precipitation. HILT data with a high-rate sampling period of 20 ms was used in our investigation. The detectors on HILT saturate at a particle flux of $10^4$ electrons $cm^{-2}s^{-1}sr^{-1}$.

The SAMPEX orbital period is ~96 minutes and the magnetic local time of the satellite repeats approximately every 80 days [*Blake et al.*, 1996]. The SAMPEX satellite's low altitude, polar orbit means that it passes through Earth's radiation belts four times with each orbit, totaling approximately 60 passes a day, at ~24 minutes a pass. SAMPEX has an orbital inclination of 81.7° [*Nakamura et al.*, 1998].

HILT mainly views the Bounce and Drift Loss Cones (BLC and DLC respectively), thus detecting electrons that will precipitate within at least one drift period (i.e., ~15 min at $L$=4 for a 1.5 MeV electron).

## 3. FAST Events

124 *Clilverd et al*. [2006] presented what is thought to be the first ever ground based detection of
125 relativistic electron microbursts. This study undertook an analysis of subionospheric VLF
126 AARDDVARK data during a magnetospheric electron flux decrease that took place at 17:10 UT
127 on the 21st of January, 2005. Short lived VLF amplitude and phase perturbations observed
128 during the flux decrease were termed FAST events. It has been reported that FAST events are
129 consistent with the expected effects of microbursts of relativistic electrons impacting on the
130 atmosphere and scattering VLF transmissions, as shown by the modelling in *Rodger et al.*
131 [2007]. Approximately 99% of individual FAST events occurring during the 21 January 2005
132 storm were not coincident across different received signals [*Clilverd et al*., 2006]. The lack of
133 event coincidence suggests that FAST events are the result of a precipitation "rainstorm"
134 producing spatially small (tens of km or less) "raindrop"-like ionisation density changes, caused
135 by a physical process spanning a much larger region, i.e., many hundreds of kilometres in
136 diameter [*Clilverd et al*., 2006], centred on or near Sodankylä.

137 A search for FAST events across the time period December 2004-June 2005 identified four
138 additional periods in SGO AARDDVARK data. As with 21 January 2005, all four additional
139 periods occurred during geomagnetic storms, with two occurring during the local day time. This
140 is expected as the relativistic electron precipitation that is thought to cause FAST event
141 signatures should penetrate so deeply into the ionosphere that they would be observable both
142 during the local day and night. The characteristics of all five documented FAST periods are
143 listed in Table 1 and an example of a single FAST event is shown in Figure 2. Included in Table
144 1 is the peak >10 MeV proton flux reported by the GOES for each period. No FAST event
145 signatures were observed for $K_P$<6, suggesting that only strong geomagnetic disturbances can
146 produce FAST events. This is consistent with the strong $D_{st}$ link previously reported between
147 storms and microbursts [*O'Brien et. al*., 2003].

148 The 21 January 2005 FAST events decayed over an average time period of 0.8 s each, while
149 those for 4-5 April 2005 were observed to decay in an average of 1.2 s each. *Rodger et al.* [2007]
150 showed the latter result is consistent with the modelled ionosphere recovery of ionization
151 increases produced at altitudes as low as 40-60 km due to REP with energies >2 MeV. The
152 shorter 21 January 2005 decay time was explained by the upper parts of the REP-produced
153 ionisation changes being "masked" by excess ionization because of proton precipitation during a
154 solar proton event. The time decays of the new FAST perturbations were examined, and
155 contrasted with the geophysical conditions at the time.

156 In Table 1 the shortest decay times are found for daytime ionospheric conditions when a solar
157 proton event was occurring (15 May 2005), while the longest were for nighttime ionospheric
158 conditions with essentially no precipitating proton flux (4-5 April 2005). A simple "cartoon
159 model" would suggest that daytime REP produced ionization would have shorter decay times
160 than that for nighttime REP. Similarly, REP produced ionization occurring during solar proton
161 events would also have shorter decay times than non-SPE periods, due to increased high-altitude
162 ionization levels perturbing the ionosphere. The FAST event decay times in Table 1 are
163 consistent with the cartoon model of a rainstorm of REP microbursts.

164 **4. SAMPEX microbursts**

165 To investigate whether FAST events are caused by relativistic electron microbursts, a survey
166 was undertaken of microbursts detected by the SAMPEX's HILT instrument during the FAST
167 periods identified. The survey was confined to REP detected while HILT was viewing the
168 bounce-loss cone exclusively, as these microbursts represent local precipitation. This was
169 defined by periods for which the mirror altitude of the SAMPEX-reported electron fluxes were
170 less than 120 km, indicating that the SAMPEX was only viewing the bounce loss cone.

171 In the current study we use the 100 km altitude projection of SAMPEX's geomagnetic field
172 line, as this provides the coordinates where any SAMPEX observed REP would precipitate into
173 the atmosphere. As relativistic electron microbursts occur during large geomagnetic storms,
174 some uncertainties might be expected in the field line mapping. We used the
175 Definite/International Geomagnetic Reference Field (DGRF/IGRF), employing the GEOPACK
176 software routines calculated for April 2005, to trace from the geomagnetic latitude and longitude
177 of SAMPEX's location, down the magnetic field line to the top of the atmosphere. The effective
178 top of the atmosphere was taken to be ~100 km, as in the SAMPEX data. To test the effect of a
179 geomagnetic storm upon the 100 km altitude field line position, the $K_P$-dependent Tsyganenko
180 magnetospheric field model was used [*Tsyganenko*, 1989]. The model was supplied with the
181 maximum $K_P$ during the 4-5 April 2005 FAST period ($K_P$=7). This showed that the maximum
182 displacement was <1 km, thus the field line mapping to the atmosphere is sufficiently accurate
183 for the purpose of this investigation.

184 To determine whether a SAMPEX reported flux increase can be identified as a microburst, two
185 criteria were employed as suggested by *O'Brien et. al.* [2004]. It was required that HILT
186 recorded a flux increase lasting <1 s before decaying back to the level of the background flux, as
187 well as measuring above a specified threshold flux during the increase. We follow *O'Brien et. al.*
188 [2004] and set the threshold flux increase, $J$, is $\sqrt{10}$ times the background population, $J_0$, that
189 SAMPEX records, i.e.,

190 $$J \geq \text{sqrt}(10) \times J_0 = 3.16\, J_0$$

191 We also use O'Brien's method of establishing the baseline flux as the $10^{th}$ percentile of the
192 fluxes, while also placing a floor at a flux level of $10^1$ cm$^{-2}$ str$^{-1}$ s$^{-1}$ [*O'Brien et. al.*, 2004]. Any
193 deviations from the $J$(DLC) level may represent bounce loss cone precipitation.

We follow the approach outlined in *Rodger et al.* [2010] to examine the radiation belt electron populations observed by SAMPEX's HILT instrument. SAMPEX orbital datafiles include the IGRF-determined pitch angle at the spacecraft of a particle heading down the instrument boresight, which have been processed to produce a world map of median pitch angles with a 1° latitude/longitude resolution. Using the IGRF model for an average SAMPEX altitude of 494 km, we have created a similar world map for the angular width of the bounce and drift loss cones at the satellite. When these are combined with the HILT boresight pitch angle width of 68° we can describe the geographical variation of the particle populations detected, taking into account the HILT viewing width.

Figure 3 presents a world map of the changing radiation belt population observed by HILT. In this figure "T" indicates trapped flux, "DLC" is drift-loss cone, and "FL BLC" is field line bounce loss cone. Note that the FL BLC angle is defined as the largest of the two loss cone angles defined for the two hemispheres. Near the geomagnetic equator the instrument only measures fluxes inside the bounce-loss cone (FL BLC), i.e., precipitating beneath the spacecraft, but for most of the globe it observes a mix of DLC and BLC populations [*Klecker et. al*., 1993; *Nakamura et. al*., 2000]. Note that above the SAMA the instrument detects part of the BLC, all of the DLC and a fraction of the trapped population. In contrast, in the Northern Hemisphere from about 85°W to 55°E the HILT detects only BLC fluxes, consistent with statements by *Li et al.* [1997]. While Figure 3 was made for the satellite mean altitude of 494 km, very similar plots are produced for the full range of altitudes over which SAMPEX orbits (~450-530 km).

A survey of SAMPEX's HILT data found relativistic electron microbursts to occur during each of the FAST periods identified in the subionospheric data. These microbursts were sorted by their northern hemisphere mirror altitude to determine whether they were in the local drift or

bounce loss cones, with the total number of microbursts detected and the number of those that were detected while viewing the BLC shown in Table 2. There is no simple relationship between the number of SGO FAST events and SAMPEX microbursts occurring on any given day. This is also true when considering $K_P$ and the number of microbursts, as is also seen with $K_P$ and the number of FAST events.

The *L*-variation in the occurrence number and average flux of SAMPEX detected BLC microbursts in our data catalogue is shown in Figure 4. The left-hand panel shows the recorded number of microbursts in each *L*-value range, which is in agreement with previously published results [*Millan and Thorne*, Fig. 5(b), 2007]. The right-hand panel shows the *L*-variation in the HILT reported BLC microburst intensities, in terms of the median increase in flux relative to the background. The dotted line shows the absolute flux increase with units of $\log_{10}$(electrons $cm^{-2}s^{-1}str^{-1}$), while the solid line shows the relative flux increase. A typical BLC microburst event observed in this study had a median >1.05 MeV flux of ~400 el. $cm^{-2}s^{-1}str^{-1}$, and was ten times larger than the background flux. Note that the mean flux increases are considerably larger, due to the very wide distribution of intensities. For example, the relative mean flux increase is 45 times above background for our BLC microburst events.

## 5. Microburst Characteristics

To investigate the link between FAST events and REP microbursts, the BLC microbursts catalogued in this study were compared with the occurrence times of all SGO FAST events in our study period. For two events to be considered as coincident in time, the peak perturbations of the events must be separated by less than the average microburst duration, which we found to be <0.29 s. The percentage of temporal overlap of the two perturbations is not used as a criterion for determining coincident occurrence because the rise and fall of a FAST event appears to be determined by ionospheric conditions and can be partially masked by multiple FAST events

occurring in a short time period. From a total of 219 BLC microbursts and 829 SGO FAST events, only two microbursts were found to be coincident with a FAST event, leading to a coincidence rate of ~1%.

Periods of SAMPEX microbursts and SGO FAST events were also compared to look for event "patterns"; to test if there was a time offset in the SAMPEX data set and to see if any groups of events appeared to be coincident in time if the time-axis was moved linearly. This effect was not seen. The drift loss cone microbursts catalogued were also tested to search for any one-to-one time correlations with FAST events, but none were found.

### 5.1 Microburst size

To determine the spatial extent of an individual microburst, two point measurements of the same microburst are needed. These two point measurements must be coincident in time and would ideally be separated by ≤10 km, the previous SAMPEX-derived estimate for the horizontal extent of a single REP microburst [*Blake et. al.*, 1996]. If the SAMPEX size estimate is correct, two measurements that are coincident in time but separated by a greater distance will not detect the same microburst, but could give some insight into the maximum possible microburst size. Hence, points coincident in time but separated by a distance of up to 20 km will be considered in this study.

In order to obtain two spatially close, temporally coincident point measurements for our study, SAMPEX must be reporting microbursts while passing over a monitored VLF transmission path, during a period in which FAST events are observed. Of the five FAST periods identified in our study, only one SAMPEX pass was found to meet these conditions. At ~3 UT on 5 April 2005, microbursts were detected while SAMPEX was viewing only the BLC on fieldlines which map to the atmosphere over the VLF transmitter-receiver path from ICV to SGO, as shown in Figure 5. The green crosses in Figure 5 are the field line traced positions of the 24 BLC microbursts that

SAMPEX detected while it travelled north-east, crossing over the VLF transmission path (marked in black) and passing near the SGO receiver (marked by a red diamond). Thirteen of these 24 BLC microbursts were detected when SAMPEX was ≤20 km from the ICV path, hence these 13 fall within our criteria for "closeness". The two closest BLC microbursts occur at distances of 4.2 km and 4.3 km away from the path from ICV to SGO. However, no FAST events are observed at SGO coincident with these two microbursts, or for any of the other 11 of this set. The SGO observations of transmissions from ICV for this time period are shown in the upper panel of Figure 6. Vertical thin lines mark the times of the first ten SAMPEX observed BLC microbursts for this time period. Clearly, no coincident FAST events are seen at these times. To provide context, the lower panel of this Figure presents examples of FAST events on this transmitter signal, which occurred approximately one hour earlier. The ten microbursts shown in the upper panel of Figure 6 have a median flux of ~3900 el. $cm^{-2}$ $s^{-1}$ $str^{-1}$, a value ~10 times greater than that found in Section 4. Even though the fluxes of these microbursts greatly exceed the typical flux we have identified, no coincident FAST events were seen. One interpretation of the lack of coincidence between BLC microbursts and FAST events in this case is that individual microbursts have radii <4 km; this estimate assumes that microbursts are roughly circular and each one is approximately the same spatial size. Our estimate is consistent with the *Blake et al*. [1996] suggestion of a diameter of <10 km, but at this point we have not been able to “catch a raindrop”.

During our analysis we also identified SAMPEX BLC microbursts that occurred on 19 January 2005, as SAMPEX was passing above western Iceland. The eastern part of Iceland hosts the US Navy VLF transmitter NRK, which is monitored at SGO and at the AARDDVARK receiver in Ny Ålesund, Svalbard (79º N, 11º E, $L$=18.3). While the NRK observations at SGO showed FAST events, those from Ny Ålesund did not, with no coincident BLC microbursts and SGO

290 FAST events. This strongly suggests that the precipitation needs to occur close to the receiver to
291 produce a detectable FAST event, as otherwise FAST events should have been seen in the data
292 from both AARDDVARK stations. In this case SAMPEX reported BLC microbursts over
293 Iceland and FAST events were reported by SGO. Given that these two points are roughly 50° in
294 longitude apart, it appears that the size of the rainstorm which produces microbursts may be very
295 large. We consider this in more detail in the next section.

296 **5.2 Storm size**

297 If the storm size, the spatial extent of the magnetospheric process that is causing microbursts,
298 is to be determined, a minimum of two point measurements are again needed. Detection of
299 microbursts occurring at similar times while being spatially separated by >10 km, would help to
300 determine the minimum size of a "microburst storm". Here we assume that FAST events are
301 indeed relativistic electron microbursts, while we acknowledge that so far, we have been unable
302 to "catch a raindrop". In this way we can attempt to measure the size of the storm driving
303 microburst production.

304 At about 14:20 UT on 8 May 2005 SAMPEX moved into the North Atlantic region in which it
305 views only the BLC. During this period, SGO had been reporting FAST events and, as expected,
306 SAMPEX detected a series of relativistic BLC microbursts as it passed from about $L$=4 to $L$=6.
307 The SAMPEX events occurred while the satellite was passing over the mouth of the Gulf of
308 Saint Lawrence in eastern Canada. The simultaneous observation of REP precipitation at
309 SAMPEX's location and SGO suggests either two widely separated storms or one single large
310 storm spanning 94° in longitude from the easternmost microburst position to SGO, stretching
311 across 5,061 km and spanning ~6-12 MLT. Further support for the existence of a single storm
312 region comes from precipitation observed on 19 January 2005. During ~1-6 UT SAMPEX
313 detected BLC microbursts over the North East coast of North America and also in the North

Atlantic. Across this time period SGO also observed FAST event activity. The fieldline traced locations of these microbursts are shown in Figure 7 as green circles, superimposed upon the orbital track for which SAMPEX is observing only the BLC (smaller blue circles). The position of SGO is shown by a red diamond. Here a single storm system of a minimum of ~90° in longitude again spanning a minimum of ~6 MLT seems most likely. Note that this is consistent with earlier SAMPEX studies which established that relativistic microbursts are most common from ~6-12 MLT [*Millan and Thorne*, Fig. 5(b), 2007], and suggests that such large storm sizes may well be typical. The MLT range and extent in which SAMPEX detects microbrsts is quite similar to that reported for chorus whistler-mode waves [*Meredith et al.*, 2003], particularly for off-equatorial locations where wave-particle interactions with relativistic electrons are possible [*Bortnik et al.*, 2007].

We are currently unable to test if a storm can be any wider, due to the fixed receiver placement at SGO and due to the restricted longitude range in which SAMPEX detects only BLC microbursts (as shown in Figure 3). In addition, we do not currently have another receiver in the AARDDVARK network in the correct longitude and *L*-range, although a new deployment is expected in western Canada in October 2010 which should allow expanded microburst storm viewing.

## 6. Discussion

Earlier work reported that FAST events detected by AARDDVARK subionospheric VLF have a one-to-one correlation of ~1-2% when observed across multiple VLF signals [*Rodger et al.*, 2007]. This very low one-to-one correlation appears to support a small scale size of ≤4 km for an individual relativistic electron microburst and also suggests that the precipitation is occurring in a “rainstorm”. There are some uncertainties concerning this interpretation, however. Previous studies have demonstrated how spatially small, highly conductive regions (produced by many

338 order of magnitude increases in D-region ionization levels) can produce high-levels of scattering
339 of subionospheric VLF transmissions [e.g., *Rodger et al.*, 1999, 2003]. One example of this
340 situation is the VLF perturbations produced by red sprites. In these cases, the ionization change
341 can be located well off the transmitter-receiver great circle path and still lead to a significant
342 VLF perturbation [*Hardman et al.*, 1998]. Extreme cases of VLF perturbations caused by
343 ionization changes occurring "behind" the receiver have been reported [*Dowden et al.*, 1996]. As
344 such, one might expect that the spatially small ionization changes produced by relativistic
345 electron microbursts would lead to FAST events irrespective of whether they are very close to
346 the transmitter-receiver great circle path or somewhere close to the receiver. In these cases, wide-
347 angle scattering would cause a single ionization change located within a few 100 km of the
348 receiver to produce coincident VLF perturbations on multiple transmitter paths. Clearly,
349 however, this is not observed in our current study. One possible reason for this is that the
350 expected maximum D-region electron density change calculated for a reasonable representation
351 of a typical relativistic electron microburst of 100 el. $cm^{-2}$ $s^{-1}$ $str^{-1}$ [*Rodger et al.*, Fig. 5, 2007] is
352 an increase of ~20-40 times, while red sprites produce 4-6 order of magnitude electron density
353 increases [e.g., *Rodger and Nunn*, 1999; *Nunn and Rodger*, 1999; *Armstrong et al.*, 2000], in
354 comparison with the ambient night-time ionosphere. This suggests that a typical relativistic
355 electron microburst is likely to be too small to lead to significant wide-angle VLF scattering.

356 During each 24 minute pass through the outer radiation belt, SAMPEX travels from $L$=4 to
357 $L$=6, the region where the majority of microbursts occur, in just 1 minute 45 s. In contrast, the
358 SGO receiver has a fixed position it can potentially detect FAST events at any time. This shows
359 up the challenge in directly comparing ground-based and satellite observations of short lived
360 events occurring only during major geomagnetic storms. However, we can use the results shown
361 in Table 2 to estimate an occurrence rate for FAST events and BLC microbursts, and thus

362 compare the two data sets more closely. During the 5 event periods FAST events are typically
363 observed at a rate of ~0.6 $min^{-1}$, while the BLC microbursts are observed at a typical rate of
364 ~8 $min^{-1}$. These estimates suggest that only ~8% of BLC microbursts are observable as FAST
365 events in the subionospheric data. This might suggest that FAST event signatures are generated
366 by the ~10% of microbursts which have the largest precipitation flux, although the lack of any
367 clear one-to-one linkage makes this suggestion quite speculative. In addition, based on the
368 occurrence rates and event duration, one would expect FAST and BLC microbursts to agree in
369 time by chance ~4% of the time. Given that the observed rate of co-incidence between FAST
370 events and BLC microbursts determined earlier in this study was ~1%, it is likely that this
371 coincidence rate is due to chance, rather than direct agreement. Thus it is not clear that we have
372 the simultaneous observation of the same relativistic precipitation bursts from SAMPEX and
373 SGO, even though both datasets indicate relativistic precipitation bursts are occurring during a
374 given time window.

375 Although the rate of occurrence of FAST events is low in comparison with BLC microbursts,
376 the SGO data does provide some additional information regarding the time variation of
377 relativistic precipitation, which is difficult to determine from low-Earth orbit satellite data alone.
378 Figure 8 is an example of the type of information that ground-based observations of relativistic
379 precipitation detected through FAST events can provide. The plot shows FAST events on the
380 transmitter NDK received at SGO from 17-22 UT on 21 January 2005. Vertical dashed lines
381 indicate the times of large solar wind pressure pulses [e.g., *Clilverd et al.*, 2007]. Two periods
382 labeled "S" represent the times of SAMPEX observations in the BLC over the $L$=3-8 range. As
383 can be seen from the plot, FAST events occur following the times of the pressure pulses, with
384 only low levels of occurrence between the two shock events. During this storm period
385 SAMPEX's orbit was such that it was unable to observe most of the time variation in the

386 relativistic microburst activity that was occurring. Clearly, continuous ground-based
387 observations can provide additional insight into the conditions required for microburst
388 generation.

389 There is currently a satellite mission in its planning stages, which aims to determine the spatial
390 extent and energy dependence of relativistic and non-relativistic electron microbursts. This
391 project is the Focused Investigations of Relativistic Electron Burst Intensity, Range, and
392 Dynamics (FIREBIRD) [*Moretto*, 2009] mission, to be launched in early 2012. A pair of
393 satellites will be launched together, each carrying a solid-state detector with a large geometric
394 factor measuring 30 keV-3 MeV electrons. The two FIREBIRD satellites will gradually drift
395 apart over the course of the mission, reaching a separation of ~300 km [*Moretto*, 2009]. The
396 FIREBIRD mission will provide a two-point microburst detection system, and as such will be a
397 further opportunity for two-point measurements of relativistic microbursts, following on from the
398 recent ground based work. Combining the FIREBIRD observations with additional ground-based
399 measurements may provide additional clarity to the storm size measurements.

400 **7. Conclusions and Summary**

401 We have attempted to show that FAST events detected in subionospheric VLF observations
402 are caused by relativistic electron microbursts, through a comparison with SAMPEX detected
403 relativistic electron precipitation occurring during FAST event periods. We have also attempted
404 to demonstrate the spatial extent of a single microburst raindrop and the size of an entire
405 microburst storm.

406 By building upon previous research into the nature of FAST events, it appears that FAST
407 events are indeed caused by relativistic electron microburst precipitation. In this study we have
408 shown that only strong geomagnetic disturbances can produce FAST events, consistent with the

409 strong $D_{st}$ link between storms and relativistic microbursts and we have shown that SAMPEX
410 detects relativistic microbursts during the identified FAST event periods. In addition, the
411 dependence of observed FAST event perturbation decay times on ionospheric conditions is also
412 consistent with the subionospheric perturbations being caused by short lived bursts of relativistic
413 electron precipitation.

414 However, this study suggests that only the strongest (i.e., highest flux) microbursts might
415 produce an observable FAST event, such that there is little direct agreement between individual
416 microbursts and FAST events. The one-to-one correlation in time between microbursts and
417 AARDDVARK FAST events is very low (~1%), and occurs most likely by chance rather than a
418 direct detection. In the one case where SAMPEX flew along a transmitter-receiver path, none of
419 the BLC microbursts reported by SAMPEX corresponded in time to FAST events. One
420 interpretation of this is that the individual microbursts have radii <4 km, which is consistent with
421 earlier satellite-based findings. Our study strongly suggests that the magnetospheric process
422 which generates relativistic microbursts is vastly larger than the individual bursts. Two examples
423 are provided where the storm stretches ~90° in longitude and ~6 hours in MLT. This is
424 particularly important given that *Lorentzen et al*. [2001b] used a ~6 MLT estimate of microburst
425 storm size when showing that relativistic electron microbursts could flush out the entire radiation
426 belt relativistic electron population in less than a day. Our findings support this previous work,
427 which concluded that REP microbursts could be a highly significant loss mechanism for
428 relativistic electrons during geomagnetic storms.

429

430 **Acknowledgments** CJR and MAC would like to thank the International Space Science Institute
431 (ISSI) of Bern, Switzerland, for providing the environment in which this paper could be

completed. JB would like to thank Dr. T. P. O'Brien for his invaluable assistance in acquiring and reading the SAMPEX data, and NSF grant ATM-0840178 for their kind support.

## References

Armstrong, R.A., D. M. Suszcynsky, W. A. Lyons, T. Nelson, (2000). Multi-Color Photometric Measurements of Ionization and Energies in Sprites, Geophys. Res. Lett., 27, 653-656.

Baker, D. N., R. W. Klebesadel, P. R. Higbie, and J. B. Blake (1986), Highly relativistic electrons in the Earth's outer magnetosphere, 1. Lifetimes and temporal history 1979-1984, J. Geophys. Res., 91, 4265-4276.

Baker, D. N., J. B. Blake, J. D. Gorney, and P. R. Higbie (1987), Highly relativistic magnetospheric electrons: a role in coupling to the middle atmosphere?, Geophys. Res. Lett., 14, 1027.

Blake, J. B., M. D. Looper, D. N. Baker, R. Nakamura, B. Klecker, and D. Hovestadt (1996), New high temporal and spatial resolution measurements by SAMPEX of the precipitation of relativistic electrons, Adv. Space Res., 18(8), 171–186.

Bortnik, J., and R. M. Thorne (2007), The dual role of ELF/VLF chorus waves in the acceleration and precipitation of radiation belt electrons, J. Atmos. Sol. Terr. Phys., 69, 378-368.

Bortnik, J., R. M. Thorne, and N. P. Meredith (2007), Modeling the propagation characteristics of chorus using CRRES suprathermal electron fluxes, J. Geophys. Res., 112, A08204, doi:10.1029/2006JA012237.

Callis, L. B., D. N. Baker, J. B. Blake, J. D. Lambeth, R. E. Bouhner, M. Natarajan, R. W. Klebesadel, and D. J. Gorney (1991), Precipitating relativistic electrons: their long term effect on stratospheric odd nitrogen levels. J. Geophys. Res., 96, 2939.

Clilverd, M. A., C. J. Rodger, and T. Ulich (2006), The importance of atmospheric precipitation in storm-time relativistic electron flux drop outs, Geophys. Res. Lett., 33, L01102, doi:10.1029/2005GL024661.

Clilverd M. A., C. J. Rodger, R. M. Millan, J. G. Sample, M. Kokorowski, M. P. McCarthy, T. Ulich, T. Raita, A. J. Kavanagh, E. Spanswick (2007), Energetic particle precipitation into the middle atmosphere triggered by a coronal mass ejection, J. Geophys. Res., 112, A12206, doi:10.1029/2007JA012395.

Clilverd, M. A., C. J. Rodger, N. R. Thomson, J. B. Brundell, Th. Ulich, J. Lichtenberger, N. Cobbett, A. B. Collier, F. W. Menk, A. Seppälä, P. T. Verronen, and E. Turunen (2009), Remote sensing space weather events: the AARDDVARK network, Space Weather, 7, S04001, doi: doi:10.1029/2008SW000412.

Clilverd, M. A., A. Seppälä, C. J. Rodger, M. G. Mlynczak, and J. U. Kozyra (2009b), Additional stratospheric $NO_x$ production by relativistic electron precipitation during the 2004 spring $NO_x$ descent event, J. Geophys. Res., 114, A04305, doi:10.1029/2008JA013472.

Hardman, S. F., R. L. Dowden, J. B. Brundell, J. L. Bähr, Z. I. Kawasaki, and C. J. Rodger (2000), Sprite observations in the Northern Territory of Australia, J. Geophys. Res., 105(D4), 4689-4697.

Imhof, W. L., H. D. Voss, J. Mobilia, D. W. Datlowe, E. E. Gaines, J. P. McGlennon, and U. S. Inan (1992), Relativistic Electron Microbursts, J. Geophys. Res., 97(A9), 13, 829–13, 837.

Klecker, B., D. Hovestadt, M. Scholer, H. Arbinger, M. Ertl, H. Kästle, E. Künneth, P. Laeverenz, E. Seidenschwang, J. B. Blake, N. Katz, and D. Marby, (1993), HILT: a Heavy Ion Large area proportional counter Telescope for solar and anomalous cosmic rays, IEEE Trans. Geosci. Remote Sens., 31(3), 542–548, doi:10.1109/36.225520.

Li, X., D. N. Baker, M. Temerin, T. E. Cayton, E. G. D. Reeves, R. A. Christensen, J. B. Blake, M. D. Looper, R. Nakamura, and S. G. Kanekal (1997), Multisatellite observations of the outer zone electron variation during the November 3-4, 1993, magnetic storm, J. Geophys. Res., 102, 14,123-14,140.

Lorentzen, K. R., J. B. Blake, U. S. Inan, and J. Bortnik (2001a), Observations of relativistic electron microbursts in association with VLF chorus, J. Geophys. Res., 106, 6017-6027, doi:10.1029/2000JA003018.

Lorentzen, K. R., M. D. Looper, and J. B. Blake (2001b), Relativistic electron microbursts during the GEM storms, Geophys. Res. Lett., 28(13) 2573–2576.

Meredith, N. P., R. B. Horne, R. M. Thorne, and R. R. Anderson, Favored regions for chorus-driven electron acceleration to relativistic energies in the Earth's outer radiation belt, Geophys. Res. Lett., 30(16), 1871, doi:10.1029/2003GL017698, 2003.

Millan, R. M. and R. M. Thorne (2007), Review of radiation belt relativistic electron losses, J. Atmos. Sol. Terr. Phys., 69, 362-377.

Moretto, T. (2009). Update on the NSF Cubesat Program. The CEDAR Post, 56:3-4.

Nakamura, R., K. Kamei, and Y. Kamide (1998), SAMPEX observations of storm-associated electron flux variations in the outer radiation belt. J. Geophys. Res., 103(A11) 26,261–26,269.

Nakamura, R., M. Isowa, Y. Kamide, D. N. Baker, J. B. Blake, and M. Looper (2000), SAMPEX observations of precipitation bursts in the outer radiation belt, J. Geophys. Res., 103(A7), 15,875-15,885.

Nunn, D., and C. J. Rodger, 1999, Modeling the relaxation of red sprite plasma, Geophysical Research Letters, 26, 3293-3296.

O'Brien, T. P., M. D. Looper, and J. B. Blake (2004), Quantification of relativistic electron microburst losses during the GEM storms, Geophys. Res. Lett., 31, L04802, doi:10.1029/2003GL018621.

O'Brien, T. P., K. R. Lorentzen, I. R. Mann, N. P. Meredith, J. B. Blake, J. F. Fennell, M. D. Looper, D. K. Milling, and R. R. Anderson (2003), Energization of relativistic electrons in the presence of ULF power and MeV microbursts: Evidence for dual ULF and VLF acceleration, J. Geophys. Res., 108(A8), 1329, doi:10.1029/2002JA009784.

Onsager, T. G., G. Rostoker, H.-J. Kim, G. D. Reeves, T. Obara, H. J. Singer, and C. Smithtro, Radiation belt electron flux dropouts: Local time, radial, and particle-energy dependence, J. Geophys. Res., 107(A11), 1382, doi:10.1029/2001JA000187, 2002.

Reeves, G. D., K. L. McAdams, R. H. W. Friedel, and T. P. O'Brien (2003), Acceleration and loss of relativistic electrons during geomagnetic storms, Geophys. Res. Lett., 30(10), 1529, doi:10.1029/2002GL016513.

Rodger, C.J., and D. Nunn (1999), VLF scattering from red sprites: Application of numerical modelling. Radio Sci., 34, 923-932.

Rodger, C. J. (1999), Red Sprites, Upward Lightning, and VLF Perturbations, Rev. Geophys., 37(3), 317–336.

Rodger, C. J. (2003), Subionospheric VLF perturbations associated with lightning discharges, J. Atmos. Sol. Terr. Phys., 65(5), 591-606.

Rodger, C. J., M. A. Clilverd, D. Nunn, P. Verronen, J. Bortnik, and E. Turunen (2007), Storm time, short-lived bursts of relativistic electron precipitation detected by subionospheric radio wave propagation, J. Geophys. Res., 112, A07301, doi:10.1029/2007JA012347.

Rodger, C. J., M. A. Clilverd, J. Green, and M.-M. Lam (2010), Use of POES SEM-2 observations to examine radiation belt dynamics and energetic electron precipitation in to the atmosphere, J. Geophys. Res., 115, A04202, doi: 10.1029/2008JA014023.

Thorne, R. M., T. P. O'Brien, Y. Y. Shprits, D. Summers, and R. B. Horne (2005), Timescale for MeV electron microburst loss during geomagnetic storms, J. Geophys. Res., 110, A09202, doi:10.1029/2004JA010882.

Tsyganenko, N. A. (1989), Determination of magnetospheric current system parameters and development of experimental geomagnetic models based on data from IMP and HEOS satellites, Planet. Space Sci., 37:5-20.

---

J. Bortnik, Dept of Atmospheric and Oceanic Sciences, UC Los Angeles, CA 90095-1565, USA. (email: jbortnik@gmail.com)

567 M. A. Clilverd, British Antarctic Survey, High Cross, Madingley Road, Cambridge CB3 0ET,
568 England, U.K. (e-mail: macl@bas.ac.uk).
569 S. Dietrich and C. J. Rodger, Department of Physics, University of Otago, P.O. Box 56,
570 Dunedin, New Zealand. (email: sdietrich@physics.otago.ac.nz,
571 crodger@physics.otago.ac.nz)
572 T. Raita, Sodankylä Geophysical Observatory, University of Oulu, Sodankylä, Finland.
573 (email: tero.raita@sgo.fi)
574

# Tables

| Date | Day/Night | Occurrence (UT) | SPE Flux (pfu) | Decay time (s) | $K_P$ | $D_{st}$ (nT) |
|---|---|---|---|---|---|---|
| 19 Jan 2005 | Night | 01:16-06:14 | 190 | 1.04 | 6.7 | -75 |
| 21 Jan 2005 | Night | 17:12-19:50 | 374 | 0.8 | 8.0 | -99 |
| 4-5 April 2005 | Night | 20:50-02:30 | 0.5 | 1.2 | 7.0 | -79 |
| 8 May 2005 | Day | 12:55-15:16 | 0.1 | 0.84 | 8.3 | -109 |
| 15 May 2005 | Day | 02:36-09:08 | 3790 | 0.63 | 8.3 | -262 |

**Table 1.** Properties of the five FAST periods found from a survey of SGO AARDDVARK observations across December 2004-June 2005. A GOES pfu = proton flux unit = >10 MeV protons $cm^{-2}$ $str^{-1}$ $s^{-1}$.

587

| **2005** | ***Kp*** | **FAST events** | **Microbursts** | **BLC microbursts** |
|---|---|---|---|---|
| 19th January | 6.7 | 103 | 84 | 55 |
| 21st January | 8.0 | 271 | 29 | 2 |
| 4th-5th April | 7.0 | 349 | 412 | 102 |
| 8th May | 8.3 | 17 | 287 | 60 |
| 15th May | 8.3 | 89 | 43 | 0 |

588

589 **Table 2.** SAMPEX microburst occurrence numbers for the five FAST periods occurring from
590 December 2004-June 2005, as identified in this study.

591

# Figures

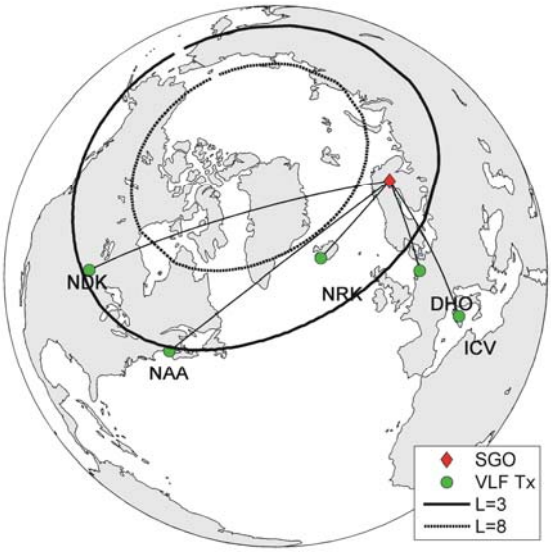


**Figure 1.** Map of the transmission paths of the five VLF signals that were used in this study. During the December 2004 – July 2005 period the AARDDVARK SGO receiver, indicated by a red diamond, was recording signals from the five transmitters that are marked by green circles. The *L*=3-8 range across which SAMPEX typically detects REP activity is enclosed between the two ellipses.

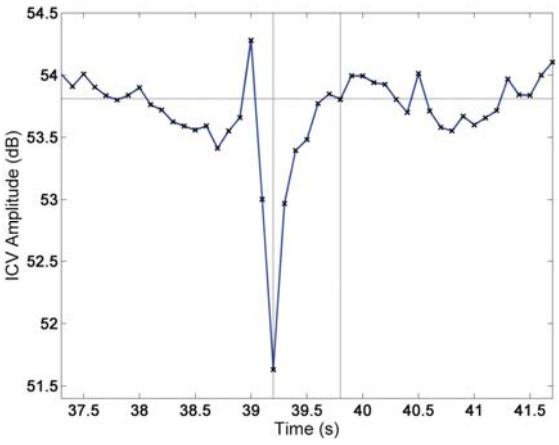


603

604 **Figure 2.** An example of a typical FAST event detected in SGO observations of ICV on 15
605 May, 2005. Here the time is given in seconds from 05:58:00 UT. The first dashed vertical line
606 at 39.2 s indicates the start of the ionisation decay, while the second vertical line at 39.8i s
607 marks the perturbations end, where the amplitude has returned to the background level.

608

609

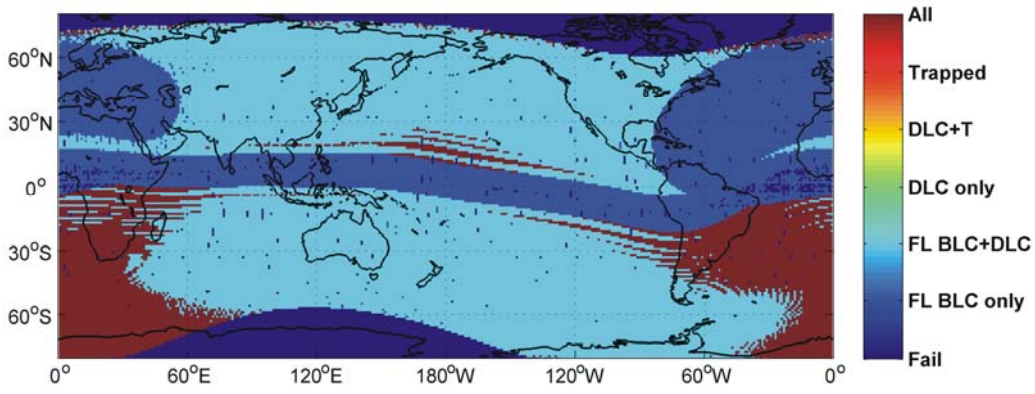


610

611 **Figure 3.** World map showing the changing radiation belt population observed by SAMPEX's
612 HILT instrument. Here T indicates trapped flux, DLC is drift-loss cone, and FL BLC is field
613 line bounce loss cone. For most locations where there is a significant radiation belt flux, it
614 observes a mix of DLC and FL BLC populations.

615

616

617

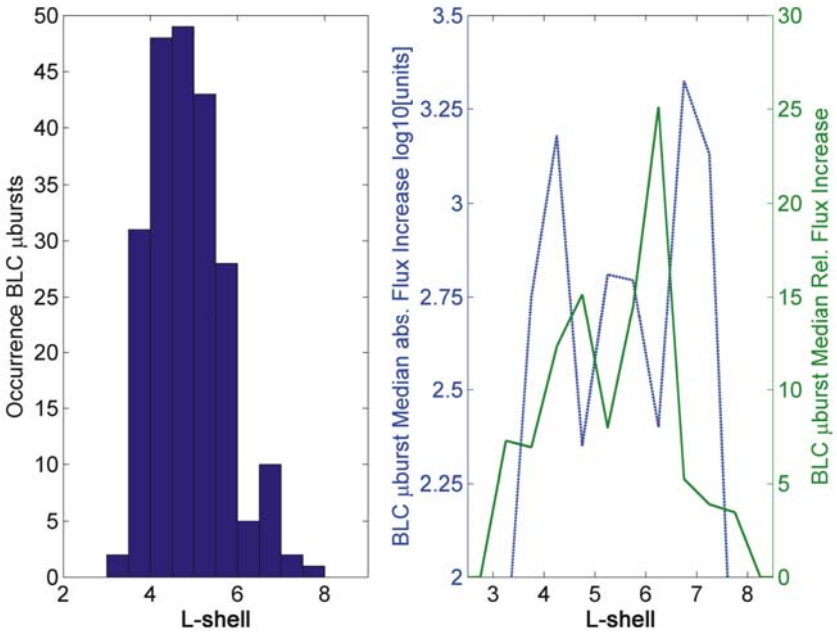


618

619 **Figure 4.** Occurrence of SAMPEX observed BLC microbursts examined in this study. The
620 variation in *L* is shown in the left-hand panel, while the right-hand panel presents the median
621 intensity of the microbursts observed. The dotted line shows the absolute flux increase with
622 units of $\log_{10}$(electrons $cm^{-2}s^{-1}str^{-1}$), while the solid line shows the relative flux increase.

623

624

625

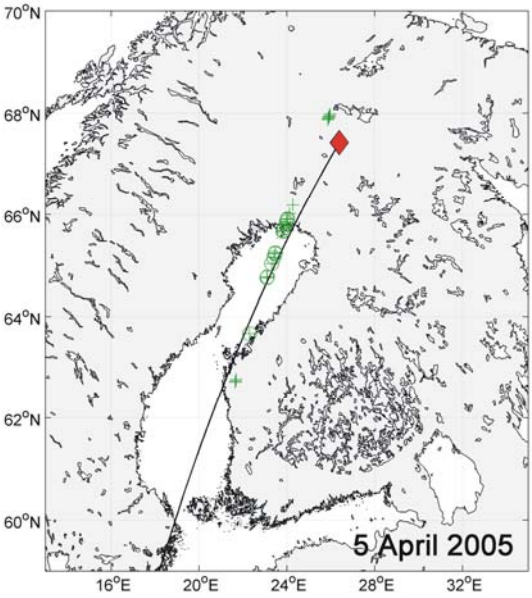


626

627 **Figure 5.** Map of the region around SGO in Finland (red diamond), showing a section of the
628 ICV transmission path in black. The green crosses mark the positions of the SAMPEX satellite
629 when it was detecting microbursts during 5 April 2005. The circled crosses are those within
630 20 km of the transmitter-receiver path.

631

632

633

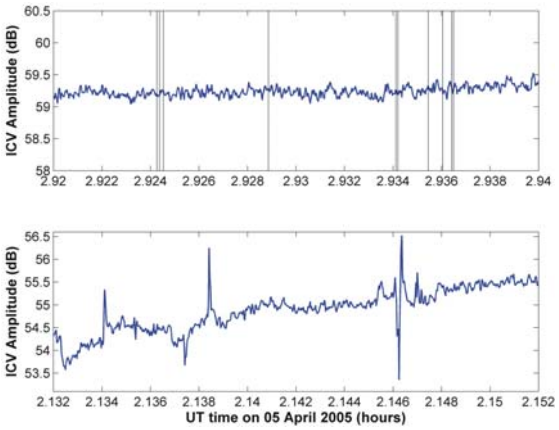


634

635 **Figure 6.** The upper panel presents the amplitude of the VLF signal from ICV received at
636 SGO during the SAMPEX observations shown in Figure 5. Vertical lines in the upper panel
637 indicate the occurrence of the ten BLC microbursts that were shown as the southern-most green
638 crosses in Figure 5. Examples of FAST events from the ICV channel are shown in the lower
639 panel.

640

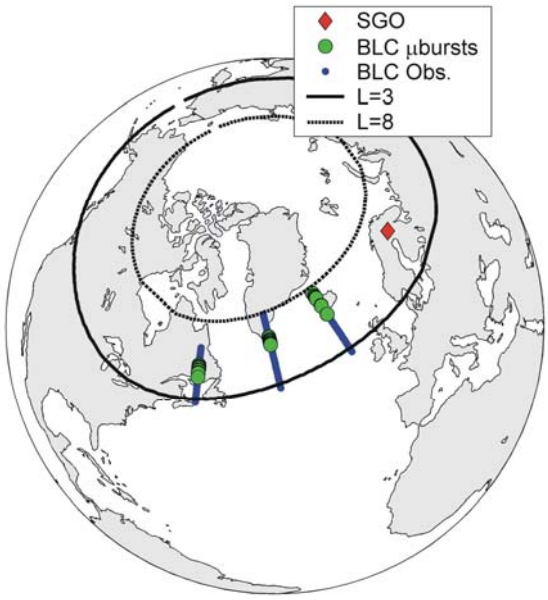


641

642 **Figure 7.** Locations of SAMPEX detected bounce loss cone microbursts (green circles) on 19
643 January 2005 which occurred in the time period FAST events were detected at SGO (red
644 diamond).

645

646

647

648

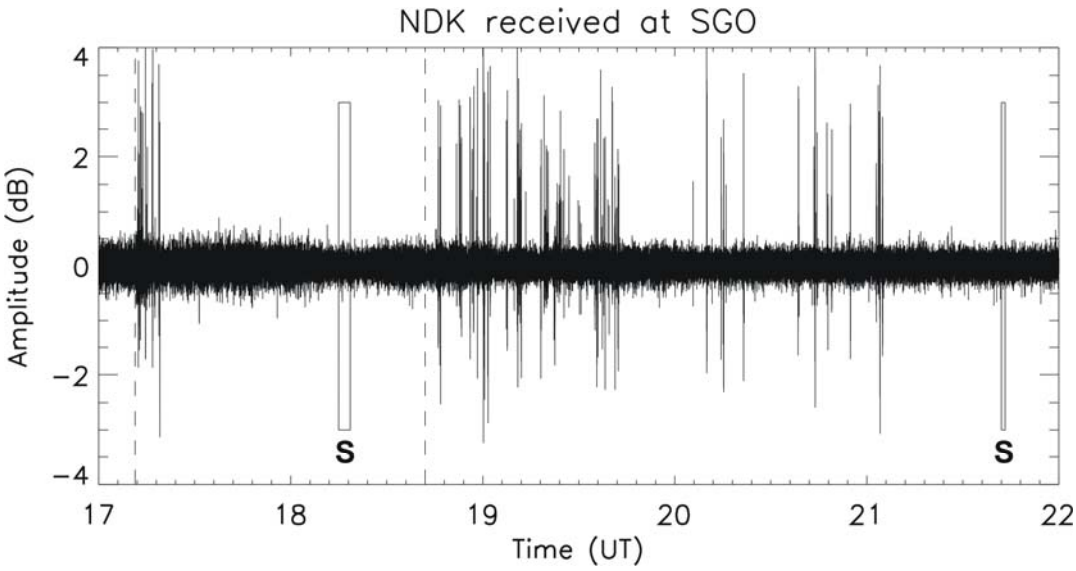


649

650 **Figure 8.** Observations of FAST events observed on transmissions from N. Dakota (NDK) at
651 Sodankylä (SGO) on 21 January 2005. The two vertical dashed lines at 17.2 UT and 18.7 UT
652 indicate the times of two solar wind pressure pulses. The two periods labeled "S" represent the
653 times of SAMPEX observations in the BLC over the *L*=3-8 range.

654